International Scholarly Research Network
ISRN Signal Processing
Volume 2012, Article ID 503707, 9 pages
doi:10.5402/2012/503707

Research Article

A Hybrid RSS/TOA Method for 3D Positioning in an Indoor Environment

Smita Tiwari, Donglin Wang, Michel Fattouche, and Fadhel Ghannouchi

The iRadio Lab, Department of Electrical and Computer Engineering, University of Calgary, Calgary, AB, Canada T2N 1N4

Correspondence should be addressed to Donglin Wang, dowang@ucalgary.ca

Received 3 October 2011; Accepted 21 November 2011

Academic Editors: D. Brie, A. Ito, and G. Ricci

This paper investigates 3D positioning in an indoor line of sight (LOS) and nonline of sight (NLOS) combined environment. It is a known fact that time-of-arrival-(TOA-) based positioning outperforms other techniques in LOS environments; however, multipath in an indoor environment, especially NLOS multipath, significantly decreases the accuracy of TOA positioning. On the other hand, received-signal-strength-(RSS-) based positioning is not affected so much by NLOS multipath as long as the propagation attenuation can be correctly estimated and the multipath effects have been compensated for. Based on this fact, a hybrid weighted least square (HWLS) RSS/TOA method is proposed for target positioning in an indoor LOS/NLOS environment. The identification of LOS/NLOS path is implemented by using Nakagami distribution. An experiment is conducted in the iRadio lab, in the ICT building at the University of Calgary, in order to (i) demonstrate the availability of Nakagami distribution for the identification of LOS and NLOS path, (ii) estimate the pass loss exponent for RSS technique, and (iii) verify our proposed scheme.

1. Introduction

In the last few years, the interest in indoor location has significantly increased due to the importance of the 3D indoor localization with a high level of accuracy. Wireless location estimation [1] is usually based on measuring one or more radio signal propagation attributes. Different attributes of a received radio signal such as time of arrival (TOA), time difference of arrival (TDOA), and angle of arrival (AOA) have been widely applied in location estimation of a target, such as a mobile station (MS) [2–6]. Unfortunately, all of the aforementioned techniques require a line of sight (LOS) link between MS and a number of base stations (BSs) of known positions. In a nonline of sight (NLOS) environment, their performances can degrade significantly.

In most indoor environments, NLOS, one of the dominant factors significantly affecting positioning accuracy, is inevitable. A variety of existing tests can identify whether a measurement fits in an LOS or a NLOS profile. Historical range measurements have been used for NLOS identification purposes in [7–9]. By applying a range scaling algorithm, the true range can be estimated by constrained minimization [7]. In [8], NLOS identification is implemented via a running variance of range estimates. Experimental results conducted in [9] indicate that the standard deviation of the range measurements in an NLOS environment is much larger than its LOS counterpart, which can also be used for identification. Another category in LOS/NLOS identification is by examining the distribution of the received signal. In a LOS channel, the TOA measurements are typically Gaussian distributed, whereas in a NLOS channel, they can be exponentially distributed [10]. Accordingly, LOS propagation can be identified by testing whether the TOA measurements have a Gaussian distribution. LOS/NLOS is identified in [11] by performing a likelihood test with prior knowledge such as kurtosis, root mean square (RMS) delay, and excess delay. The distribution function of the received power envelope is used in [12] to identify LOS/NLOS. The authors in [13] take advantage of the fact that the received power envelope in a LOS environment has a Ricean distribution, while it has a Rayleigh distribution in a NLOS environment. Using average fading duration and the level crossing rate of the power envelopes is another way to deal with LOS/NLOS identification [14]. A Nakagami-m distribution is proposed in [15] for LOS/NLOS identification, which is proved to be the optimal radio channel model in an indoor environment.

When identifying a NLOS channel, it is necessary to mitigate its effects. A method is proposed in [16] to correct NLOS range error based on the prior knowledge of the range statistics. In [17], the authors try to weight the NLOS measurements by the residue of the measured range. A hard weight selection in weighted least square (WLS) is introduced for a NLOS correction [11]. In this paper, a hybrid weighted least square (HWLS) RSS/TOA method is proposed for target positioning in an indoor LOS/NLOS environment based on the fact that (i) TOA-based positioning outperforms other techniques in LOS environments; however, multipath in an indoor environment, especially NLOS multipath, significantly decreases its accuracy. (ii) On the other hand, the received-signal-strength-(RSS-) based positioning is not affected as much by NLOS multipath as long as the propagation attenuation can be correctly estimated and the multipath effects have been compensated for. So, TOA can be applied for LOS cases while RSS can be used for NLOS cases. By conducting an indoor experiment, three objectives have been reached in this paper: (i) to demonstrate the availability of Nakagami distribution for the identification of LOS and NLOS, (ii) to estimate the pass loss exponent based on RSS data, and (iii) to verify the proposed HWLS RSS/TOA.

The paper is organized as follows. Section 2 proposes the novel 3D positioning algorithm, HWLS RSS/TOA, for LOS/NLOS environments, and derives its Cramer-Rao lower bound (CRLB). Section 3 describes our experimental setup. In Section 4, the identification of LOS/NLOS is implemented, the path loss model is estimated, and the experimental results are reported, followed by a conclusion in Section 5.

2. Proposed 3D Positioning Algorithm for LOS/NLOS Environments

2.1. Positioning Scheme in an Indoor Environment. It is a known fact that TOA-based positioning [18] outperforms other techniques such as RSS-based positioning in a LOS environment. However, multipath in a dense urban area or in an indoor environment, especially NLOS multipath, significantly decreases its accuracy. On the other hand, RSS is not affected as much by NLOS multipath as long as the propagation attenuation can be correctly estimated and the multipath effects have been compensated for. Based on these facts, we are proposing a hybrid weighted least square (HWLS) RSS/TOA method for positioning in LOS/NLOS environments, which contains the following procedure by assuming N BSs (Txs) of known positions in a wireless location network which attempts to estimate the position of MS (Rx).

(a) Initialize by setting $i = 1$.

(b) Consider the received signal from the ith BS and identify whether the direct path is LOS or NLOS using Nakagami-m distribution. If it is LOS, go to (c); otherwise, jump to (d);

(c) Use a WLS TOA for LOS range estimation. If $i = N$, jump to (f); otherwise, let $i = i+1$ and go back to (b).

(d) Estimate the propagation exponent α as well as its shadowing effect, thus obtaining a path loss model.

(e) Based on the WLS RSS proposed in Subsection 2.2 below, estimate the NLOS range. If $i = N$, go to (f); otherwise, let $i = i + 1$ and go back to (b).

(f) Implement target positioning based on all N range measurements.

2.2. Proposed 3D WLS

2.2.1. RSS. Let $\mathbf{x}_i = [x_i, y_i, z_i]^T$, $i = 1, 2, \ldots, N$, be the known coordinates for the ith BS and let $\mathbf{x} = [x, y, z]^T$ be the unknown coordinates of MS. The estimated range by means of RSS, $\hat{R}_{i_{\mathrm{RSS}}}$, between the ith BS and MS, can be modeled as

$$\hat{R}_{i_{\mathrm{RSS}}} = F_i \frac{P_i^t}{P_i^r} + \omega_i, \tag{1}$$

where P_i^r is the received power, P_i^t is the transmitted power, F_i represents an unknown but deterministic coefficient, and ω_i denotes the range error. The received power P_i^r can be further expressed as

$$P_i^r = F_i \frac{P_i^t}{d_i^\alpha}, \tag{2}$$

where α is the propagation attenuation, and d_i is the range between the ith BS and MS. Substituting (2) into (1), we have

$$\hat{R}_{i_{\mathrm{RSS}}} = \left[(x - x_i)^2 + (y - y_i)^2 + (z - z_i)^2\right]^{\alpha/2} + \omega_i. \tag{3}$$

First, let us consider a noise-free environment, where (3) can be expressed as

$$\hat{R}_{i_{\mathrm{RSS}}} = \left[(x - x_i)^2 + (y - y_i)^2 + (z - z_i)^2\right]^{\alpha/2}. \tag{4}$$

Or equivalently,

$$\hat{R}_{i_{\mathrm{RSS}}}^{2/\alpha} = x^2 + x_i^2 - 2xx_i + y^2 + y_i^2 - 2yy_i + z^2 + z_i^2 - 2zz_i. \tag{5}$$

Furthermore,

$$xx_i + yy_i + zz_i - 0.5Q = \frac{1}{2}\left(x_i^2 + y_i^2 + z_i^2 - \hat{R}_{i_{\mathrm{RSS}}}^{2/\alpha}\right), \tag{6}$$

where Q is defined as

$$Q = x^2 + y^2 + z^2. \tag{7}$$

In matrix notation, (6) can be expressed as

$$G\Theta = H, \tag{8}$$

where

$$G \triangleq \begin{bmatrix} x_1 & y_1 & z_1 & -0.5 \\ \vdots & \vdots & \vdots & \vdots \\ x_N & y_N & z_N & -0.5 \end{bmatrix},$$

$$H \triangleq \frac{1}{2}\begin{bmatrix} x_1^2 + y_1^2 + z_1^2 - \hat{R}_{1_{\text{RSS}}}^{2/\alpha} \\ \vdots \\ x_N^2 + y_N^2 + z_N^2 - \hat{R}_{N_{\text{RSS}}}^{2/\alpha} \end{bmatrix}, \tag{9}$$

and the unknown variable

$$\Theta \triangleq \begin{bmatrix} x \\ y \\ z \\ Q \end{bmatrix}.$$

Now considering a noisy environment as in (3), (8) is replaced by

$$\omega = G\Theta - H, \tag{10}$$

where the range error vector is $\omega \triangleq [\omega_1, \omega_2, \ldots, \omega_N]^T$. By minimizing the range error ω, the least square (LS) solution gives an estimate of Θ as

$$\hat{\Theta}_{\text{LS}_{\text{RSS}}} = \arg\min_{\Theta}(G\Theta - H)^T(G\Theta - H) = \left(G^TG\right)^{-1}G^TH. \tag{11}$$

To enhance its estimation accuracy, a weighted matrix W is used in (11) so that $\hat{\Theta}_{\text{LS}_{\text{RSS}}}$ satisfies the fundamental constraint given in (7), and (11) is replaced by

$$\begin{aligned} \hat{\Theta}_{\text{WLS}_{\text{RSS}}} &= \arg\min_{\Theta}(G\Theta - H)^T W_{\text{RSS}}(G\Theta - H) \\ &= \left(G^T W_{\text{RSS}} G\right)^{-1} G^T W_{\text{RSS}} H, \end{aligned} \tag{12}$$

where $W_{\text{RSS}} = SJS$, $S \triangleq \text{diag}\,[d_{1_{\text{RSS}}}^{2-\alpha}/\alpha,\ d_{2_{\text{RSS}}}^{2-\alpha}/\alpha, \ldots,\ d_{N_{\text{RSS}}}^{2-\alpha}/\alpha]$, $J \triangleq \text{diag}\,[\sigma_{1_{\text{RSS}}}^2, \sigma_{2_{\text{RSS}}}^2, \ldots, \sigma_{N_{\text{RSS}}}^2]$, and $\sigma_{i_{\text{RSS}}}^2$, $i = 1, 2, \ldots, N$, is the estimation variance using RSS.

2.2.2. TOA. The 2D LS TOA is derived in [19]. Appendix 5 extends it to the 3D WLS TOA case. In Appendix 5, WLS TOA is used instead of LS TOA in order to enhance its estimation accuracy in a LOS environment.

2.3. CRLB for the Proposed Scheme. The CRLB for 2D TOA positioning is derived in [19]. By using a similar derivation, the CRLB for 3D TOA positioning can be obtained as

$$\text{CRLB}_{\text{WLS}_{\text{TOA}}}(\hat{\mathbf{x}}) = \left\{ E \begin{bmatrix} \sum_{i=1}^{N} \frac{(x-x_i)^2}{2\sigma_i^2 d_i^2} & \sum_{i=1}^{N} \frac{(x-x_i)(y-y_i)}{2\sigma_i^2 d_i^2} & \sum_{i=1}^{N} \frac{(x-x_i)(z-z_i)}{2\sigma_i^2 d_i^2} \\ \sum_{i=1}^{N} \frac{(x-x_i)(y-y_i)}{2\sigma_i^2 d_i^2} & \sum_{i=1}^{N} \frac{(y-y_i)^2}{2\sigma_i^2 d_i^2} & \sum_{i=1}^{N} \frac{(y-y_i)(z-z_i)}{2\sigma_i^2 d_i^2} \\ \sum_{i=1}^{N} \frac{(x-x_i)(z-z_i)}{2\sigma_i^2 d_i^2} & \sum_{i=1}^{N} \frac{(y-y_i)(z-z_i)}{2\sigma_i^2 d_i^2} & \sum_{i=1}^{N} \frac{(z-z_i)^2}{2\sigma_i^2 d_i^2} \end{bmatrix} \right\}^{-1}, \tag{13a}$$

and for each dimension, we have

$$\text{CRLB}_{\text{WLS}_{\text{TOA}}}(x) = \left[\text{CRLB}_{\text{WLS}_{\text{TOA}}}(\hat{\mathbf{x}})\right]_{11}, \tag{13b}$$

$$\text{CRLB}_{\text{WLS}_{\text{TOA}}}(y) = \left[\text{CRLB}_{\text{WLS}_{\text{TOA}}}(\hat{\mathbf{x}})\right]_{22}, \tag{13c}$$

$$\text{CRLB}_{\text{WLS}_{\text{TOA}}}(z) = \left[\text{CRLB}_{\text{WLS}_{\text{TOA}}}(\hat{\mathbf{x}})\right]_{33}, \tag{13d}$$

while the CRLB for 3D RSS positioning can be obtained as

$$\text{CRLB}_{\text{WLS}_{\text{RSS}}}(\hat{\mathbf{x}}) = \left\{ E \begin{bmatrix} \sum_{i=1}^{N} \frac{(x-x_i)^2}{2\sigma_i^2 d_i^{2(2-\alpha)}} & \sum_{i=1}^{N} \frac{(x-x_i)(y-y_i)}{2\sigma_i^2 d_i^{2(2-\alpha)}} & \sum_{i=1}^{N} \frac{(x-x_i)(z-z_i)}{2\sigma_i^2 d_i^{2(2-\alpha)}} \\ \sum_{i=1}^{N} \frac{(x-x_i)(y-y_i)}{2\sigma_i^2 d_i^{2(2-\alpha)}} & \sum_{i=1}^{N} \frac{(y-y_i)^2}{2\sigma_i^2 d_i^{2(2-\alpha)}} & \sum_{i=1}^{N} \frac{(y-y_i)(z-z_i)}{2\sigma_i^2 d_i^{2(2-\alpha)}} \\ \sum_{i=1}^{N} \frac{(x-x_i)(z-z_i)}{2\sigma_i^2 d_i^{2(2-\alpha)}} & \sum_{i=1}^{N} \frac{(y-y_i)(z-z_i)}{2\sigma_i^2 d_i^{2(2-\alpha)}} & \sum_{i=1}^{N} \frac{(z-z_i)^2}{2\sigma_i^2 d_i^{2(2-\alpha)}} \end{bmatrix} \right\}^{-1}. \tag{14}$$

Assume in our indoor experiment that there are M LOS BSs out of N BSs, for example, the ith BS, $1 \le i \le M$, corresponds to a LOS link between itself and MS, while the jth BS, $M + 1 \le j \le N$, corresponds to a NLOS link. In other words, our proposed method has M TOA measurements and N-M RSS measurements. Therefore, using a similar derivation as [19], the CRLB for the proposed HWLS RSS/TOA can be expressed as

$$\mathrm{CRLB}_{\mathrm{WLS}_{\mathrm{RSS}}}(\hat{\mathbf{x}}) = \left\{ E\left[\begin{array}{ccc} \dfrac{\partial^2 \ln(p(r \mid \mathbf{x}))}{\partial x^2} & \dfrac{\partial^2 \ln(p(r \mid \mathbf{x}))}{\partial x \partial y} & \dfrac{\partial^2 \ln(p(r \mid \mathbf{x}))}{\partial x \partial z} \\ \dfrac{\partial^2 \ln(p(r \mid \mathbf{x}))}{\partial x\, \partial y} & \dfrac{\partial \ln(p(r \mid \mathbf{x}))}{\partial y^2} & \dfrac{\partial^2 \ln(p(r \mid \mathbf{x}))}{\partial y\, \partial z} \\ \dfrac{\partial^2 \ln(p(r \mid \mathbf{x}))}{\partial x \partial z} & \dfrac{\partial^2 \ln(p(r \mid \mathbf{x}))}{\partial y \partial z} & \dfrac{\partial \ln(p(r \mid \mathbf{x}))}{\partial z^2} \end{array} \right] \right\}^{-1}, \tag{15a}$$

where

$$\frac{\partial^2 \ln(p(r \mid \mathbf{x}))}{\partial x^2} = \sum_{i=1}^{M} \frac{(x - x_i)^2}{2\sigma_i^2 d_i^2} + \sum_{i=M+1}^{N} \frac{(x - x_i)^2}{2\sigma_i^2 d_i^{2(2-\alpha)}}, \tag{15b}$$

$$\frac{\partial^2 \ln(p(r \mid \mathbf{x}))}{\partial y^2} = \sum_{i=1}^{M} \frac{(y - y_i)^2}{2\sigma_i^2 d_i^2} + \sum_{i=M+1}^{N} \frac{(y - y_i)^2}{2\sigma_i^2 d_i^{2(2-\alpha)}}, \tag{15c}$$

$$\frac{\partial^2 \ln(p(r \mid \mathbf{x}))}{\partial z^2} = \sum_{i=1}^{M} \frac{(z - z_i)^2}{2\sigma_i^2 d_i^2} + \sum_{i=M+1}^{N} \frac{(z - z_i)^2}{2\sigma_i^2 d_i^{2(2-\alpha)}}, \tag{15d}$$

$$\frac{\partial^2 \ln(p(r \mid \mathbf{x}))}{\partial x \partial y} = \sum_{i=1}^{M} \frac{(x - x_i)(y - y_i)}{2\sigma_i^2 d_i^2} + \sum_{i=M+1}^{N} \frac{(x - x_i)(y - y_i)}{2\sigma_i^2 d_i^{2(2-\alpha)}}, \tag{15e}$$

$$\frac{\partial^2 \ln(p(r \mid \mathbf{x}))}{\partial x \partial z} = \sum_{i=1}^{M} \frac{(x - x_i)(z - z_i)}{2\sigma_i^2 d_i^2} + \sum_{i=M+1}^{N} \frac{(x - x_i)(z - z_i)}{2\sigma_i^2 d_i^{2(2-\alpha)}}, \tag{15f}$$

$$\frac{\partial^2 \ln(p(r \mid \mathbf{x}))}{\partial y \partial z} = \sum_{i=1}^{M} \frac{(y - y_i)(z - z_i)}{2\sigma_i^2 d_i^2} + \sum_{i=M+1}^{N} \frac{(y - y_i)(z - z_i)}{2\sigma_i^2 d_i^{2(2-\alpha)}}. \tag{15g}$$

3. Experimental Site and Setup

3.1. Experimental Site. To validate the proposed scheme in a realistic environment, an indoor experiment is conducted in the iRadio Lab, in the ICT building, at the University of Calgary. The 3D experimental site is shown in Figure 1. Its size is approximately equal to 18.0 m × 7.0 m × 3.5 m. The Lab is divided into three sections: (1) Section 1 is a small room, that is, 3.0 m × 4.0 m, located at the entrance of the laboratory, (2) Section 2 is its main body, and (3) Section 3 is a small conference room partitioned from the lab's main body.

The outer wall of the lab is glass-walled, which is a big source for signal reflecting. There are a couple of metallic

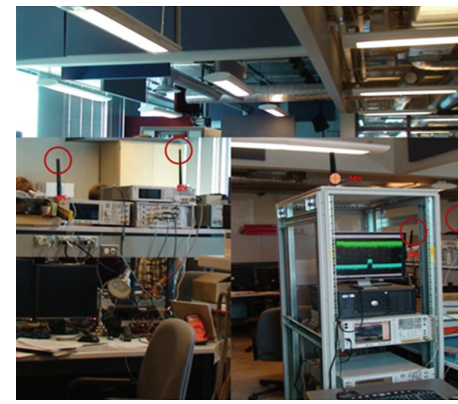

Figure 1: Experiment site in the iRadio lab, ICT Building at University of Calgary.

heating pipes located around the room ceiling. The lab is equipped with many electronics instruments, computers, WiFi devices, scanners, printers, furniture, and metal cabinets. Polished furniture can generate signal reflection. For the LOS scenario, all BSs and MS are placed in the 2nd part of the lab, while for the NLOS scenario, the NLOS BSs are placed in the 1st Section and the 3rd Section. In Section 3, the receiver is kept where a NLOS situation is guaranteed. In Figure 1, all BSs and MS are marked with red circles.

3.2. Experimental Setup. The whole system architecture of this experiment is depicted in Figure 2. Each BS is specified by using the Agilent vector signal generator (VSG) N5182A capable of generating probing signal up to 4 GHz. The output parameter of the VSG is selected based on the technical specification of the analog front-end board MAX2830 Evaluation Kit from Maxim, and an agile digital signal processing (DSP) unit. The overall technical specification used in this study is summarized in Table 1.

MATLAB/ADS is used to generate an OFDM signal, which is then upload to the VSG at 2.45 GHz carrier frequency, a 5 MHz bandwidth, and an 89.6 MHz sampling frequency. The VSG is connected to an RF switch with 5 outputs, each of which is further connected to a high gain omnidirection antenna using a coaxis cable. All BSs are clock-synchronized. The receiving antenna is directly

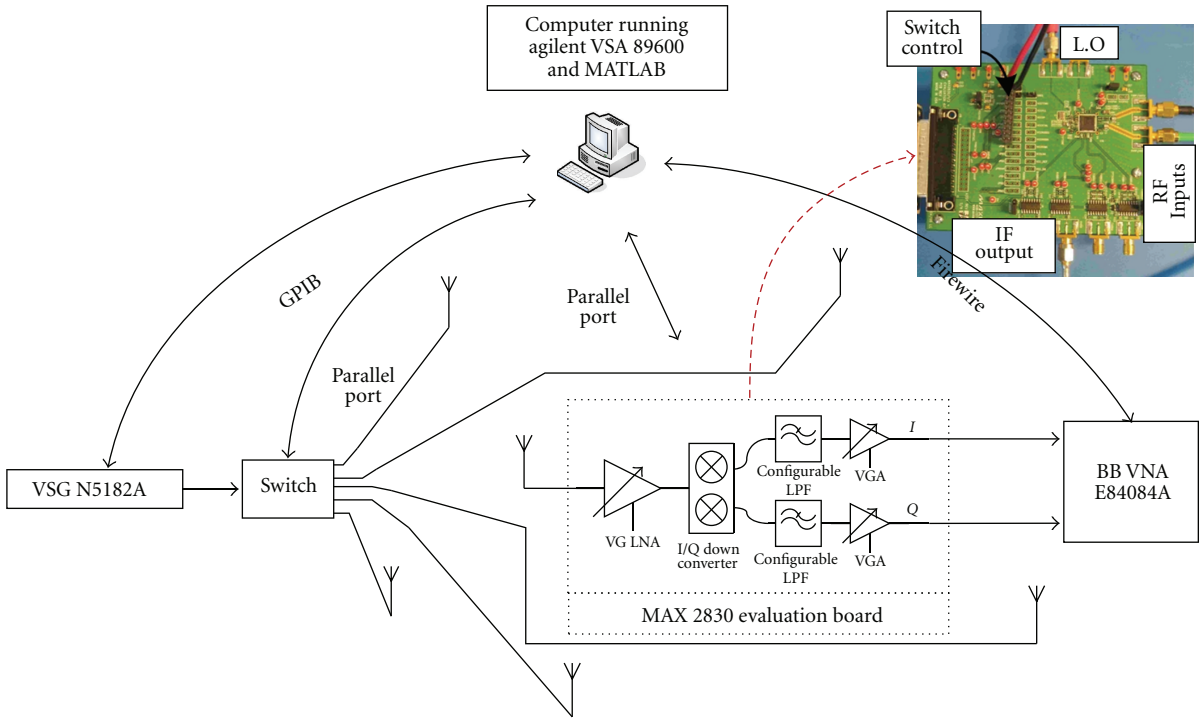

Figure 2: Test bed for 3D indoor location.

Table 1: Technical specification for analog front-end board from maxim (max 2830 evaluation kit) used in experiment.

Specification	Technical detail
Analog front end band	2.4 GHz–2.5 GHz
Rx noise figure	3.3 dB
Rx sensitivity	−75 dBm
Rx I/Q gain	0.1 dB
Rx phase imbalance	0.35
Based band gain control range	33–62 dB

connected to the Maxim board. The front-end is composed of a variable gain low-noise amplifier (LNA) followed by an I/Q zero-IF down converter, a programmable lowpass filter (LPF), and a variable gain amplifier (VGA) as shown in Figure 2. After downconversion, the baseband signal is sampled and quantified by an analog-to-digital converter. A MATLAB program is then used to capture both the I component and the Q component from the front end. The estimated time delay is obtained at the output of a matched filter, where the known time-multiplexed at the RF switch and the extra cable delay are considered for time delay compensation.

4. Empirical Result

4.1. Demonstration of Nakagami Distribution for LOS/NLOS Identification. As mentioned in [15], Nakagami distribution outperforms Rician distribution and Rayleigh distribution for LOS/NLOS identification because it is a more general form [15]. The following experiment verifies the availability of the Nakagami distribution for LOS identification, which is the first of our three objectives.

The probability density function (PDF) of Nakagami distribution is given by

$$f(r) = \frac{2m^m r^{2m-1}}{\Gamma(m)\Omega^m} \exp\left\{-\frac{mr^2}{\Omega}\right\} \quad r \geq 0, \tag{13}$$

where $\Gamma(m)$ is the Gamma function, Ω, which is equal to $E\{r^2\}^2$, denotes the second moment, and $m \geq 1/2$, which is referred to as a shape factor, is defined as

$$m = \frac{E^2\{r^2\}}{E\left\{[r^2 - E(r^2)]^2\right\}}. \tag{14}$$

The corresponding cumulative density function (CDF) can be expressed as

$$F(r) = P\left(\frac{mr^2}{\Omega}, m\right), \tag{15}$$

where $P(\cdot)$ is the incomplete Gamma function. In the special case, when $m = 1$, the Nakagami distribution behaves as a Rayleigh distribution. When $m > 1$, it behaves as a Rician distribution. When $m = 0.5$, it behaves as a one-sided Gaussian distribution.

In our experiment, two BSs are assumed to be in a NLOS environment while three BSs are assumed to be in a LOS environment. 100 observations are captured from each BS, followed by an m-detector test to identify whether each observation belongs to a LOS environment or a NLOS

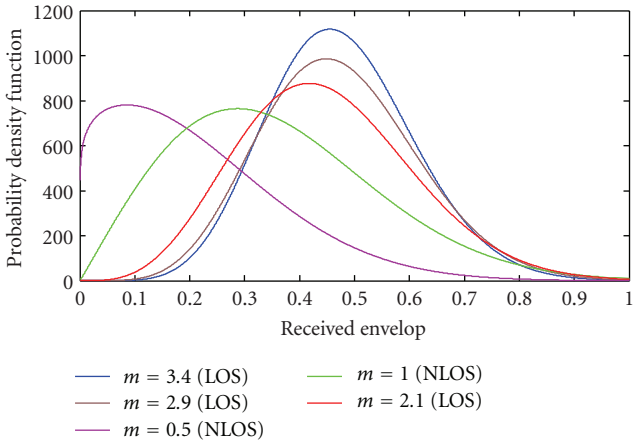

Figure 3: PDF of LOS/NLOS channels and their corresponding Nakagami-m factors.

Table 2: Passing rate of chi-square and K-S hypothesis tests.

Measurements	Chi-square	K-S Test
LOS	85.6412	76.06
NLOS	82.7933	75.71

one. One m is estimated from these 100 observations. For instance, Figure 3 shows several typical PDFs, their corresponding m factor values, and their corresponding channel types, that is, LOS or NLOS, where one can see that when $m \leq 1$, the channel is NLOS, and when $m > 1$, the channel is LOS.

To demonstrate the availability of the Nakagami distribution for LOS/NLOS identification, both a Kolmogorov-Smirnov (K-S) test and Chi-square test are performed at 5% significance level. Table 2 illustrates their passing rate. One can see that the Nakagami m-factor has a 75% above passing rate for both tests. However, the passing rate of a LOS channel is shown to be higher than a NLOS one for both tests. This demonstrates that the LOS/NLOS channel can be properly identified using a Nakagami distribution for our indoor environment.

4.2. Path Loss Model Estimation. Another objective in our experiment is to estimate the path loss exponent and shadowing effects of the experimental site. To generate this model, we measure the distance between each BS and MS as well as the received signal power. For a LOS test, we place all BSs in the lab's Section 2, select fifteen different positions for MS, and measure their received signal powers and their distances between each BS and MS. At each MS position, we stored a minimum of 20 signal power measurements and then move MS to another position. The same process is repeated for tests in a NLOS environment.

Figure 4 shows all received power measurements and its line of fit for pass loss exponent estimation in a LOS environment. Similarly, Figure 5 shows all received power measurements and its line of fit for pass loss exponent

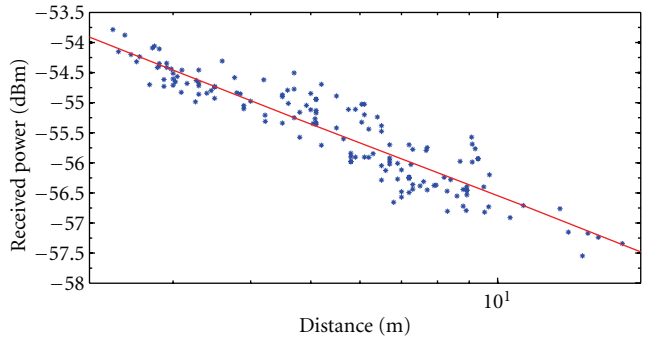

Figure 4: Path loss exponent estimation in a LOS environment.

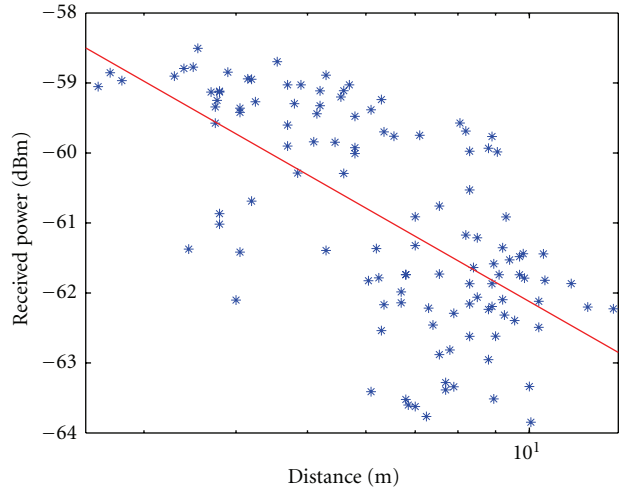

Figure 5: Path Loss Exponent Estimation in a LOS and NLOS combined environment.

Table 3: Estimated path loss exponent and shadowing effect.

Indoor Environment	Path Loss Exponent	Shadowing Effect
LOS	1.7	2.2
NLOS	3.2	2.7

estimation in a NLOS environment. Table 3 illustrates the estimated path loss exponent and shadowing effect for both LOS and NLOS environments, where one can see that in a LOS environment, the path loss exponent and shadowing effect are found to be equal to 1.7 and 2.2, respectively; in a NLOS environment, the path loss exponent and shadowing effect are 3.2 and 2.7, respectively.

4.3. Verification of Our Proposed HWLS RSS/TOA. The third objective of our experiment is to verify our proposed HWLS RSS/TOA for the indoor NLOS environments. For this purpose, (1) MS is placed in the lab's 2nd Section; (2) two BSs are placed in the lab's 1st Section and the 3rd Section, leading to a NLOS propagation channel and; three BSs are placed in the lab's 2nd Section, leading to a LOS propagation channel. 100 observations are captured for this scenario.

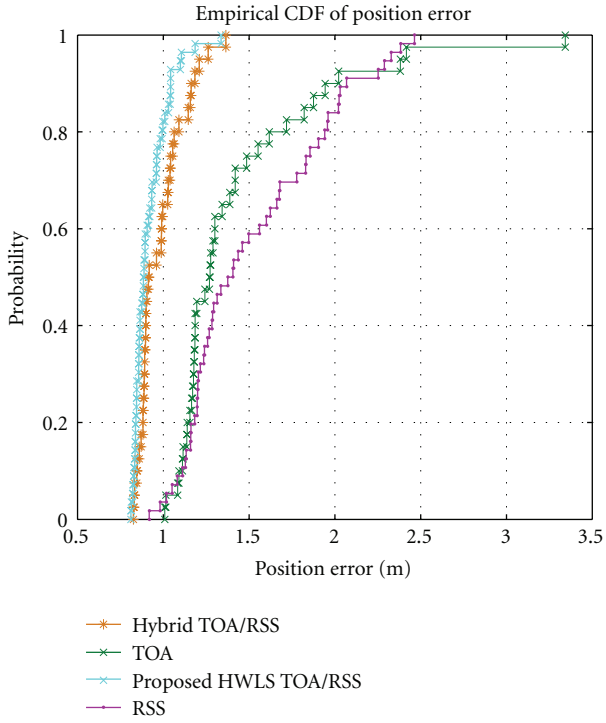

Figure 6: CRLB for positioning estimation using TOA alone, RSS alone, hybrid RSS/TOA and the proposed HWLS RSS/TOA.

Using the derivation given in ((13a), (13b), (13c), and (13d)) through (15f), together with [19], all CRLBs for positioning estimation using 3D TOA alone, 3D RSS alone, 3D hybrid RSS/TOA, and our proposed 3D HWLS RSS/TOA are plotted in Figure 6 for comparison. One can see that the proposed 3D HWLS RSS/TOA outperforms all other three methods. Furthermore, the CDF of the root mean square error (RMSE) for positioning estimation using 3D TOA alone, 3D RSS alone, 3D hybrid RSS/TOA, and our proposed 3D HWLS RSS/TOA is shown in Figure 7, which is obtained from an indoor LOS/NLOS environments. Figure 7 indicates that the proposed HWLS RSS/TOA provides the best positioning accuracy compared to all other three methods. The overall performance of the considered methods for 3D positioning estimation is reported in Table 4, where a 2.02 m RMSE can be obtained by the proposed HWLS RSS/TOA, compared to 4.23 m by Hybrid RSS/TOA, 5.75 m by TOA alone, and 6.10 m by RSS alone.

5. Conclusion

In this paper, a novel HWLS RSS/TOA method has been proposed for target localization in an indoor NLOS environment. An experiment is conducted in the iRadio lab, in the ICT building at the University of Calgary, to demonstrate our proposed algorithm. Experimental results indicated that HWLS exhibits a much better performance than TOA alone, RSS alone, and hybrid RSS/TOA in terms of positioning accuracy in an indoor LOS/NLOS environment.

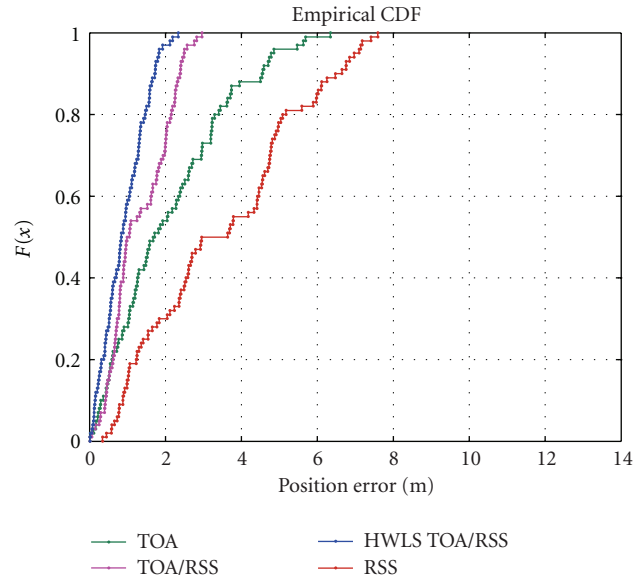

Figure 7: CDF of positioning error using TOA alone, RSS alone, hybrid RSS/TOA, and the proposed HWLS RSS/TOA.

Appendix

Derivation of 3D WLS TOA

Let $\mathbf{x}_i = [x_i, y_i, z_i]^T$ be the known coordinates of the ith BS and let (x, y, z) be the unknown coordinates of MS. The true distance, d_i, between the ith BS and MS can be expressed as [20–22]

$$d_i = \sqrt{(x - x_i)^2 + (y - y_i)^2 + (z - z_i)^2}. \quad (A.1)$$

In a noisy environment, the estimated range, $\hat{R}_{i_{\text{TOA}}}$, by TOA estimation can be given as

$$\hat{R}_{i_{\text{TOA}}} = d_i + \omega_i, \quad (A.2)$$

where ω_i denotes the range error. In the absence of range error, we have

$$\hat{R}_{i_{\text{TOA}}} = d_i = \sqrt{(x - x_i)^2 + (y - y_i)^2 + (z - z_i)^2}. \quad (A.3)$$

Therefore,

$$\hat{R}^2_{i_{\text{TOA}}} = x^2 + x_i^2 - 2xx_i + y^2 + y_i^2 - 2yy_i + z^2 + z_i^2 - 2zz_i. \quad (A.4)$$

Furthermore,

$$xx_i + yy_i + zz_i - 0.5Q = \frac{1}{2}\left(x_i^2 + y_i^2 + z_i^2 - \hat{R}^2_{i_{\text{TOA}}}\right), \quad (A.5)$$

where $Q \triangleq x^2 + y^2 + z^2$. In matrix notation, we have

$$G\Theta = H, \quad (A.6)$$

Table 4: Rmse for 3D positioning error using TOA alone, RSS alone, hybrid RSS/TOA and hwls RSS/TOA.

Method	Coordinates	Variance (m)	Min Error (m)	Mean Error (m)	RMSE (m)
TOA	X	1.50	1.023	1.04	5.75
	Y	0.70	1.068	1.05	
	Z	1.80	1.12	1.38	
RSS	X	1.75	1.34	1.80	6.1
	Y	1.20	1.90	1.72	
	Z	2.01	1.40	2.40	
Hybrid TOA/RSS	X	1.44	0.98	1.00	4.23
	Y	0.50	0.97	0.99	
	Z	1.50	1.01	1.20	
HWLS TOA/RSS	X	0.013	0.43	0.45	2.02
	Y	0.012	0.15	0.20	
	Z	0.28	0.119	0.72	

where G and Θ are the same as (9), while the matrix is

$$H \triangleq \begin{bmatrix} x_1^2 + y_1^2 + z_1^2 - \hat{R}_{1_{\text{TOA}}}^2 \\ \vdots \\ x_N^2 + y_N^2 + z_N^2 - \hat{R}_{N_{\text{TOA}}}^2 \end{bmatrix}. \tag{A.7}$$

Now considering a noisy case, we have

$$\omega = G\Theta - H, \tag{A.8}$$

where the range error vector is $\omega \triangleq [\omega_1, \omega_2, \ldots, \omega_N]^T$. By minimizing the rang error ω, the least square (LS) solution estimates Θ as

$$\hat{\Theta}_{\text{LS}_{\text{TOA}}} = \arg\min_{\Theta}(G\Theta - H)^T(G\Theta - H) = \left(G^T G\right)^{-1} G^T H. \tag{A.9}$$

To enhance its estimation accuracy, a weighted matrix W is used in (A.9) so that $\hat{\Theta}_{\text{LS}_{\text{RSS}}}$ satisfies the fundamental constraint given. Using this idea, the WLS RSS estimates Θ as

$$\begin{aligned} \hat{\Theta}_{\text{WLS}_{\text{TOA}}} &= \arg\min_{\Theta}(G\Theta - H)^T W_{\text{TOA}}(G\Theta - H) \\ &= \left(G^T W_{\text{TOA}} G\right)^{-1} G^T W_{\text{TOA}} H, \end{aligned} \tag{A.10}$$

where $W_{\text{TOA}} \triangleq SJS$, $S \triangleq \text{diag}\,[d_{1_{\text{TOA}}}, d_{2_{\text{TOA}}}, \ldots, d_{N_{\text{TOA}}}]$, $J \triangleq \text{diag}\,[\sigma_{1_{\text{TOA}}}^2, \sigma_{2_{\text{TOA}}}^2, \ldots, \sigma_{N_{\text{TOA}}}^2]$, and $\sigma_{i_{\text{TOA}}}^2$, $i = 1, 2, \ldots, N$, is the variance of $\hat{\Theta}_{\text{WLS}_{\text{TOA}}}$ using TOA estimation.

Acknowledgments

This work is supported by the Alberta Informatics Circle of Research Excellence (iCORE), the Natural Sciences and Engineering Research Council of Canada (NSERC), the Canada Research Chair (CRC) Program, TRLabs, and the Cell-Loc Location Technologies Inc.

References

[1] D. Wang, *Multicarrier transmission for wireless location—range estimation and positioning*, Ph.D. dissertation, Electrical Engineering Dept., University of Calgary, Calgary, Canada, 2010.

[2] J. Caffery and G. L. Stuber, "Subscriber location in CDNA cellular networks," *IEEE Transactions on Vehicular Technology*, vol. 47, no. 2, pp. 406–416, 1998.

[3] D. Wang and M. Fattouche, "OFDM transmission for time-based range estimation," *IEEE Signal Processing Letters*, vol. 17, no. 6, article 69, pp. 571–574, 2010.

[4] K. Yu, J. P. Montillet, A. Rabbachin, P. Cheong, and I. Oppermann, "UWB location and tracking for wireless embedded networks," *Signal Processing*, vol. 86, no. 9, pp. 2153–2171, 2006.

[5] D. Wang and M. Fattouche, "Multipath mitigation for LOS TBRE using NDB OFDM transmission and phase correlation," *Electronics Letters*, vol. 46, no. 21, pp. 1467–1468, 2010.

[6] D. Wang, M. Fattouche, and F. M. Ghannouchi, "Fundamental limit of OFDM range estimation in a separable multipath environment," *Circuits, Systems, and Signal Processing*. In press.

[7] S. Venkatraman, J. Caffery, and H. R. You, "Location using LOS range estimation in NLOS environments," in *Proceedings of the Vehicular Technology Conference (VTC '02)*, pp. 856–860, May 2002.

[8] J. Borras, P. Hatrack, and N. B. Mandayam, "Decision theoretic framework for NLOS identification," in *Proceedings of the 48th IEEE Vehicular Technology Conference (VTC '98)*, pp. 1583–1587, May 1998.

[9] M. P. Wylie and J. Holtzman, "Non-line of sight problem in mobile location estimation," in *Proceedings of the 5th IEEE International Conference on Universal Personal Communications (ICUPC '96)*, pp. 827–831, October 1996.

[10] S. Venkatraman and J. Caffery, "Statistical approach to non-line of- sight BS identification," in *Proceedings of the International Symposium on Wireless Personal Multimedia Communications (WPMC '02)*, pp. 296–300, October 2002.

[11] I. Güvenç, C. C. Chong, F. Watanabe, and H. Inamura, "NLOS identification and weighted least-squares localization for UWB systems using multipath channel statistics," *EURASIP Journal on Advances in Signal Processing*, vol. 2008, no. 36, pp. 1–14, 2008.

[12] S. Venkatesh and R. M. Buehrer, "Non-line-of-sight identification in ultra-wideband systems based on received signal statistics," *IET Microwaves, Antennas and Propagation*, vol. 1, no. 6, pp. 1120–1130, 2007.

[13] G. L. Stuber, *Principles of Mobile Communication*, Kluwer Academic Publishers, 1996.

[14] A. Abdi, K. Wills, H. A. Barger, M. S. Alouini, and M. Kaveh, "Comparison of the level crossing rate and average fade duration of Rayleigh, Rice, and Nakagami fading models with mobile channel data," in *Proceedings of the 52nd Vehicular Technology Conference (VTS '2000)*, pp. 1850–1857, September 2000.

[15] M. Nakagami, "The m-distribution—a general formula for intensity distribution of rapid fading," in *Proceedings of the Symposium on Statistical Methods in Radio Wave Propagation*, pp. 3–36, Pergamon Press, January 1960.

[16] M. P. Wylie and J. Holtzman, "Non-line of sight problem in mobile location estimation," in *Proceedings of the 5th IEEE International Conference on Universal Personal Communications (ICUPC '96)*, pp. 827–831, October 1996.

[17] P. C. Chen, "A non line of sight error mitigation algorithm in location estimation," in *Proceedings of the IEEE Wireless Communications and Networking Conference*, pp. 316–320, September 1999.

[18] D. Wang, H. Leung, M. Fattouche, and F. M. Ghannouchi, "Efficient spectrum allocation and TOA-based localization in cognitive networks," *Wireless Personal Communications*. In press.

[19] K. W. Cheung, H. C. So, W. K. Ma, and Y. T. Chan, "Least squares algorithms for time-of-arrival-based mobile location," *IEEE Transactions on Signal Processing*, vol. 52, no. 4, pp. 1121–1128, 2004.

[20] G. Zhao, D. Wang, M. Fattouche, and M. Jin, "Novel wireless positioning system for OFDM-based cellular networks," *IEEE Systems Journal*. In press.

[21] D. Wang, M. Fattouche, and F. M. Ghannouchi, "Geometry-based doppler analysis for GPS receivers," *Wireless Personal Communications*, vol. 62, pp. 1–13, 2011.

[22] G. Zhao, D. Wang, and M. Fattouche, "Time sum of arrival based BLUE for mobile target positioning," *Advanced Science Letters*, vol. 4, no. 1, pp. 165–167, 2011.